New Phytologist

Guard cells in fern stomata are connected by plasmodesmata, but control cytosolic Ca^{2+} levels autonomously

Lena J. Voss[1], Scott A. M. McAdam[2,3], Michael Knoblauch[4], Jan M. Rathje[1], Tim Brodribb[2], Rainer Hedrich[1] and M. Rob G. Roelfsema[1]

[1]Molecular Plant Physiology and Biophysics, Julius-von-Sachs Institute for Biosciences, Biocenter, Würzburg University, Julius-von-Sachs-Platz 2, D-97082 Würzburg, Germany; [2]School of Biological Science, University of Tasmania, Hobart, TAS 7001, Australia; [3]Botany and Plant Pathology, Purdue University, 915 West State Street, West Lafayette, IN 47907, USA; [4]School of Biological Sciences, Washington State University, PO Box 644236, Pullman, WA 99164-4236, USA

Author for correspondence:
M. Rob G. Roelfsema
Tel: +49 931 3186121
Email: roelfsema@botanik.uni-wuerzburg.de

Received: *9 August 2017*
Accepted: *6 March 2018*

New Phytologist (2018) **219:** 206–215
doi: 10.1111/nph.15153

Key words: calcium signals, ferns, guard cell, plasmodesmata, potassium channels, seed plants, stomata.

Summary

- Recent studies have revealed that some responses of fern stomata to environmental signals differ from those of their relatives in seed plants. However, it is unknown whether the biophysical properties of guard cells differ fundamentally between species of both clades.
- Intracellular micro-electrodes and the fluorescent Ca^{2+} reporter FURA2 were used to study voltage-dependent cation channels and Ca^{2+} signals in guard cells of the ferns *Polypodium vulgare* and *Asplenium scolopendrium*.
- Voltage clamp experiments with fern guard cells revealed similar properties of voltage-dependent K^+ channels as found in seed plants. However, fluorescent dyes moved within the fern stomata, from one guard cell to the other, which does not occur in most seed plants. Despite the presence of plasmodesmata, which interconnect fern guard cells, Ca^{2+} signals could be elicited in each of the cells individually.
- Based on the common properties of voltage-dependent channels in ferns and seed plants, it is likely that these key transport proteins are conserved in vascular plants. However, the symplastic connections between fern guard cells in mature stomata indicate that the biophysical mechanisms that control stomatal movements differ between ferns and seed plants.

Introduction

The development of stomata was a major step in the evolution of land plants, as these adjustable pores in the leaf surface allow plants to restrict water loss (Berry *et al.*, 2010; Raven & Edwards, 2014; Brodribb & McAdam, 2017). In periods of limited precipitation, plants reduce their transpiration by closure of their stomata, whereas these pores open under favorable growth conditions to enable CO_2 uptake for photosynthesis (Hetherington & Woodward, 2003; Kollist *et al.*, 2014). Stomata are thus of key importance in adaptive responses to changes in environmental conditions and, consequently, are a major topic of interest in plant biology.

In accordance with their main function, stomata of seed plants open in response to light and low atmospheric CO_2 levels and close in response to low air humidity (Shimazaki *et al.*, 2007; Kim *et al.*, 2010; Bauer *et al.*, 2013; Kollist *et al.*, 2014). In contrast with the well-studied stomata of seed plants, our knowledge about their counterparts in bryophytes and early-branching vascular plants (ferns and lycophytes) is still fragmentary, and the evolution of stomatal function, to some extent, has been controversially discussed (Roelfsema & Hedrich, 2016). For instance, several studies have found that the drought hormone abscisic acid (ABA) closes stomata of mosses, lycophytes and ferns (Chater *et al.*, 2011, 2016; Ruszala *et al.*, 2011; Horak *et al.*, 2017), but other experiments on lycophytes and ferns have revealed that the stomata of these species are ABA insensitive (Brodribb & McAdam, 2011; McAdam & Brodribb, 2012; Duckett & Pressel, 2018).

Stomata of ferns have also been found to differ from those in seed plants, with respect to blue light-specific opening responses (Doi & Shimazaki, 2008; Doi *et al.*, 2015). In *Arabidopsis* and several other seed plants, phototropins serve as blue light-activated protein kinases that provoke stomatal opening by the activation of plasma membrane H^+-ATPases and the inhibition of anion channels in guard cells (Marten *et al.*, 2007a; Shimazaki *et al.*, 2007; Hiyama *et al.*, 2017). This phototropin-dependent response was found to be absent in guard cells of the fern clade *Polypodiopsida*, whereas it was present in other clades of ferns (Doi & Shimazaki, 2008; Doi *et al.*, 2015). Therefore, the ability of phototropins to stimulate stomatal opening is likely to have evolved in early land plants, but has been lost in the *Polypodiopsida*.

A common feature of the stomata of all land plants, including ferns, is their ability to open in response to photosynthetically active radiation (PAR) (Doi *et al.*, 2015). In seed plants, the PAR response is closely linked to CO_2 sensing by guard cells (Roelfsema *et al.*, 2002, 2006; Kollist *et al.*, 2014). In line with the

interrelation of PAR and CO_2 responses, fern stomata open in response to a drop in atmospheric CO_2 concentration from 350 to 100 ppm, as in seed plants (Brodribb *et al.*, 2009). However, stomata of ferns fail to close when the atmospheric CO_2 level is increased from 350 to 600 ppm, whereas this stimulus induces stomatal closure in seed plants (Brodribb *et al.*, 2009). In a later study of Franks & Britton-Harper (2016), higher atmospheric CO_2 concentrations were used (800 ppm), which induced the closure of fern stomata, albeit at a much lower velocity than in seed plants (Roelfsema & Hedrich, 2016).

Although differences in the stomatal responses of ferns and seed plants have received attention in a number of recent studies (Franks & Britton-Harper, 2016; Brodribb & McAdam, 2017; Cai *et al.*, 2017), little attention has been paid to the potential variation in the biophysical properties of stomata. Studies with histochemical K^+ stains in the 1970s indicated that the guard cells of ferns accumulate K^+ during stomatal opening (Stevens & Martin, 1977; Lösch & Bressel, 1979). However, apart from these early studies, little is known about ion transport in fern guard cells. We therefore used microelectrodes, in combination with Ca^{2+}-sensitive dyes, to study voltage-dependent cation transport and Ca^{2+} signaling in ferns.

Materials and Methods

Plant material

Polypodium vulgare and *Asplenium scolopendrium* were obtained from the botanical garden in Würzburg, Germany. *Polypodium glycyrrhiza* was obtained from the botanical garden in Göttingen and originated from the Columbia River Gorge (Oregon, USA), or was collected in the Columbia River Gorge. *Ceratopteris richardii* (line Hnn) was grown from spores obtained from Purdue University (West Lafayette, IN, USA) and *Selaginella uncinata* was received from the University of Bristol (Bristol, UK). All plants were cultivated in glasshouses and additional light was supplied by HQL-pressure lamps (Philips, http://www.lighting.philips.com; Powerstar HQI-E, 400 W) with a day : night cycle of 12 h : 12 h. All experiments were conducted with stomata in newly unfurled leaves.

Setup for impalement of microelectrodes and electrical configuration

Intracellular microelectrode experiments were conducted with intact plants (*P. vulgare*, *A. scolopendrium* and *S. uncinata*), whole fronds provided with water through the cut off petiole (Lucifer Yellow injection into *P. vulgare* and *P. glycyrrhiza*) or leaf disks (*C. richardii*) kept in the following bath solution (5 mM KCl, 0.1 mM $CaCl_2$ and 5 mM potassium citrate, pH 5.0). The adaxial side of fronds was attached with double-sided adhesive tape to a Plexiglas holder in the focal plane of an upright microscope (Axioskop 2FS, Zeiss, http://www.zeiss.com). Stomata were visualized with water immersion objectives (W Plan-Apochromat, ×40/0.8 or ×63/1.0, Zeiss) dipped into a drop of bath solution placed on the abaxial frond surface. Microelectrodes were impaled into guard cells with a piezo-driven micro-manipulator (MM3A, Kleindiek Nanotechnik, http://www.nanotechnik.com). All microelectrodes were prepared from borosilicate glass capillaries with filament (inner diameter, 0.58 mm; outer diameter, 1.0 mm; Hilgenberg, http://www.hilgenberg-gmbh.com). Double- and triple-barreled microelectrodes were made from two or three capillaries, which were aligned, heated and twisted 360°, and pre-pulled on a customized vertical electrode puller (L/M-3P-A, Heka, http://www.heka.com). Subsequently, microelectrode tips were pulled on a horizontal laser puller (P 2000; Sutter Instruments Co., http://www.sutter.com).

The voltage recording and current injection barrels of double- and triple-barreled electrodes were filled with 300 mM KCl. The tips of the dye injection barrels were filled with 10 mM Oregon Green 488 1,2-bis(o-aminophenoxy)ethane-N,N,N′,N′-tetraacetic acid (BAPTA-1) (hexapotassium salt), 1 mM Lucifer Yellow or 20 mM FURA2, whereas the remaining of these barrels were filled with 300 mM KCl. All barrels of the electrodes were connected via Ag/AgCl half cells to custom-made headstages with an input resistance of $> 10^{11}$ Ohm. The reference electrodes were made from glass capillaries filled with 300 mM KCl and plugged with a salt bridge (2% agarose and 300 mM KCl), which were connected to Ag/AgCl half cells and placed in the bath solution.

The headstages were connected to a custom-made amplifier (Ulliclamp01) with an integrated differential amplifier, which enabled voltage clamp measurements. Voltage steps were controlled by PULSE software (Heka) using an LIH-1600 interface (Heka). The data were low-pass filtered at 10 Hz with a four-pole, low-pass, Bessel filter (LPF 202A; Warner Instruments Corp., www.warneronline.com) and sampled at 100 Hz.

Fluorescence microscopy

Bright field and fluorescence microscopy images were obtained with a charge multiplying CCD camera (QuantEM, Photometrics, http://www.photometrics.com/) mounted on an Axioskop 2FS microscope (Zeiss). Transmitted light was provided by the microscope lamp, whereas Lucifer Yellow and Oregon Green-BAPTA (OG-BAPTA) were excited with light from an Hg/metal halide lamp (HXP120, Leistungselektronic JENA, http://www.lej.de), which was filtered through a bandpass filter of 430/24 nm (Lucifer Yellow, ET 430/24, Chroma Technology Corp., https://www.chroma.com) or of 472/30 nm (OG-BAPTA, 472/30 nm, BrightLine, Semrock, http://www.semrock.com). A dichroic mirror (495 nm LP) guided the excitation light through the objectives (W Plan-Apochromat, ×40/0.8, or ×63/1.0, Zeiss), whereas the fluorescent light was filtered with an emission bandpass filter (520/30 nm, BrightLine, Semrock). The filters could be rapidly exchanged within a spinning disk confocal unit (CARV II, Crest Optics, http://www.crestopt.com), which was mounted on the camera port of the upright microscope. Fluorescence images with OG-BAPTA were made with the confocal spinning disk, whereas it was moved out of the light path in experiments with Lucifer Yellow and FURA2.

The fluorescent calcium indicator dye FURA2 was excited with 200-ms UV-flashlight pulses at 345 nm and 390 nm

wavelengths and time intervals of 1 s or 3 s using a VisiChrome high-speed polychromator system (Visitron Systems, Puchheim, Germany, www.visitron.de). The FURA2 emission signal was passed through a dichroic mirror (FT 395; Zeiss) and was filtered with a 510 nm bandpass filter (D510/40M, Chroma Technology Corp.). All fluorescence measurements were conducted with the aid of the VISIVIEW software package (Visitron Systems).

Image analysis and calibration

Fluorescent images were analyzed offline with the IMAGEJ software package (National Institutes of Health, Bethesda, MD, USA; http://imagej.nih.gov/ij/). The image stacks of OG-BAPTA, Lucifer Yellow and FURA2 were corrected for background fluorescence and drift using the 'Registration/StackReg' plugin of IMAGEJ. Ratio images of OG-BAPTA were calculated relative to the image obtained at the start of the experiment. A mask was applied to FURA2 image stacks, which blacked out areas in which the fluorescence intensity was close to, or below, the background value. Differential values between the image stacks obtained with excitation light of 345 and 390 nm were calculated with the 'Calculator plus' module or 'Ratio Plus' plugin of IMAGEJ.

FURA2 *F*345/*F*390 ratio images were calibrated to obtain values for the cytosolic free Ca^{2+} concentration, according to the procedure of Grynkiewicz *et al.* (1985). For this purpose, the minimal FURA2 ratio value was obtained by clamping guard cells to 0 mV and current injecting FURA2 simultaneously with BAPTA, with triple-barreled electrodes, the third barrel of which was filled with 20 mM FURA2 and 500 mM BAPTA. The maximal fluorescence intensity was achieved by clamping FURA2 loaded cells to −260 mV and simultaneously moving the microelectrode in and out of the cell with the micromanipulator. The dissociation constant (K_d) of FURA2, required for calibration (Grynkiewicz *et al.*, 1985), had previously been determined in intact guard cells (Levchenko *et al.*, 2005).

Electron microscopy

Leaf sections were microwave fixed at 750 W for 3 min on ice with a temperature limit of 35°C in 2% paraformaldehyde and 2% formaldehyde in 0.1 M cacodylate buffer. Post-fixation was performed with 2% OsO_4 for 2 h at room temperature. The samples were dehydrated in a graded methanol series of 10% increments on ice in the microwave at 750 W for 1 min each step. After transfer into propylene oxide, samples were embedded into Spurr's resin, sectioned and studied with a FEI T-20 transmission electron microscope (FEI Co., Hillsboro, Oregon, USA, https://www.fei.com).

Results

The conductance of fern guard cells is dominated by voltage-dependent ion channels

In seed plants, the uptake and release of K^+ cause changes in the osmotic pressure of guard cells, which lead to stomatal

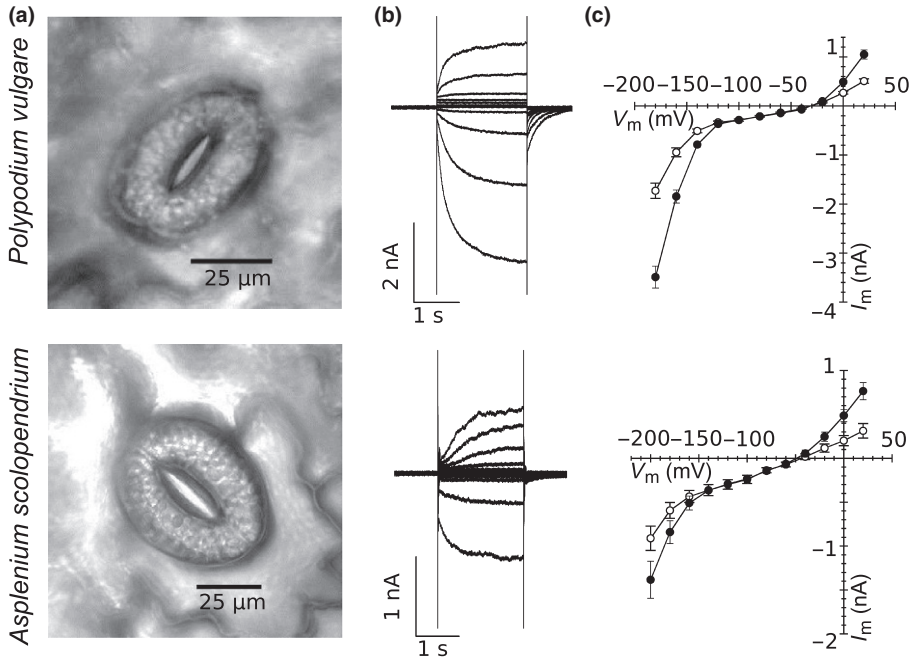

Fig. 1 Ion channels in guard cells of the ferns *Polypodium vulgare* (upper panels) and *Asplenium scolopendrium* (lower panels). (a) Bright field images of fern stomata; note the large number of chloroplasts in the guard cells of both *P. vulgare* and *A. scolopendrium*. (b) Voltage-induced activation of ion channels in fern guard cells. Guard cells were impaled with double-barreled microelectrodes and the membrane potential was clamped from a holding potential of −100 mV, in 2-s pulses and with 20-mV steps, to more positive or negative values. Current traces are superimposed. Note that the time-dependent changes in ion currents display all hallmarks of K^+ efflux and uptake channels, known from seed plant guard cells. (c) Current–voltage relation of fern guard cells, determined at the start (open symbols) and end (closed symbols) of 2-s test pulses applied from a holding potential of −100 mV as shown in (b). Average data are shown ($n = 40$, *P. vulgare*; $n = 15$, *A. scolopendrium*); error bars, ± SE.

movements (Roelfsema & Hedrich, 2005). In *Arabidopsis*, two types of K^+ channels were found in the plasma membrane of guard cells, which opened at voltages that enabled either the uptake or release of K^+ (Very & Sentenac, 2002; Roelfsema & Hedrich, 2005; Hedrich, 2012). However, little is known about voltage-dependent channels of ferns, and we therefore impaled double-barreled electrodes filled with 300 mM KCl into guard cells of *P. vulgare* and *A. scolopendrium*. One barrel of these electrode pairs was used to measure the plasma membrane potential and the other to inject ion currents (Fig. 1). Voltage pulses were applied from a holding potential of −100 mV, in 20 mV steps, to + 20 mV, which caused the slow activation of outward ion currents (Fig. 1b,c), reminiscent of those conducted by Guard cell Outward Rectifying K^+ channel (GORK) in *Arabidopsis* (Ache *et al.*, 2000; Very & Sentenac, 2002). Likewise, voltage pulses to more negative voltages (−180 and −200 mV for *P. vulgare* and *A. scolopendrium*, respectively) led to ion currents with instantaneous and time-dependent components (Fig. 1b,c), suggesting the activation of K^+ channels, similar to K^+ channel in Arabidopsis thaliana ½ (KAT½) of *Arabidopsis* (Szyroki *et al.*, 2001; Roelfsema & Hedrich, 2005).

Ca^{2+}-permeable channels in fern guard cells

Although K^+ channels facilitate a major pathway for rapid changes in the osmotic potential of guard cells, Ca^{2+} channels probably play an important role in the regulation of stomatal movements (Dodd *et al.*, 2010; Kudla *et al.*, 2010; Roelfsema & Hedrich, 2010). In guard cells of seed plants, cytosolic Ca^{2+} signals can be evoked by the application of hyperpolarizing voltage pulses (Grabov & Blatt, 1998; Levchenko *et al.*, 2005; Stange *et al.*, 2010). These voltage pulses can either stimulate Ca^{2+}-permeable channels in the guard cell plasma membrane (Hamilton *et al.*, 2000; Pei *et al.*, 2000) or trigger Ca^{2+} release from intracellular stores (Voss *et al.*, 2016). We tested whether these Ca^{2+} release mechanisms can also be triggered with hyperpolarizing voltage pulses in fern guard cells by impaling guard cells of *P. vulgare* with triple-barreled electrodes. Two barrels of the electrodes were used to apply voltage pulses, whereas the Ca^{2+}-sensitive dye OG-BAPTA, or FURA2, was current injected via the third barrel (Levchenko *et al.*, 2008; Voss *et al.*, 2016).

OG-BAPTA was used in combination with a spinning disk confocal system to study Ca^{2+} signals in a narrow focal plane (Voss *et al.*, 2016). The fluorescence of OG-BAPTA in guard cells was compared with the values measured at the start of the experiment and shown as ratio images (Fig. 2a; Supporting Information Movie S1). Single-step voltage pulses of 10 s, from a holding potential of −100 mV to −200 mV, elicited a transient elevation of the cytosolic Ca^{2+} level (Fig. 2a; Movie S1), as described previously for *Vicia faba* and tobacco (Grabov & Blatt, 1998; Levchenko *et al.*, 2005; Stange *et al.*, 2010).

In addition to OG-BAPTA, the Ca^{2+} reporter FURA2 was used to determine the absolute changes in the cytosolic free Ca^{2+} concentration evoked by voltage pulses (Fig. 2b–d). The 10-s voltage pulses caused an average rise of the cytosolic free Ca^{2+} concentration of 250 nM and the Ca^{2+} level returned to its prestimulus value in *c.* 100 s (Fig. 2b,c; Movie S2). The strength of the Ca^{2+} signal was dependent on the magnitude of the voltage pulse applied (Fig. 2d). It is likely that these Ca^{2+} signals are evoked by Ca^{2+}-permeable channels in the plasma membrane and intracellular stores, as shown recently for tobacco (Voss *et al.*, 2016).

In the majority of cells (19 of 27 cells), the rise in the Ca^{2+} concentration started at a position close to the site of impalement (Fig. 2b; Movie S2), whereas it first arose at a position away from the impalement site in the remaining cells (eight of 27 cells) (Fig. S1; Movie S3). The voltage pulses thus seem to preferentially activate a Ca^{2+} release mechanism close to the site of impalement, but the activation of Ca^{2+} sources at a further distance can also occur.

Guard cells of *A. scolopendrium* were also loaded with OG-BAPTA and stimulated with 10-s voltage pulses to −200 mV. As in *P. vulgare*, these voltage pulse triggered a transient elevation of the cytosolic Ca^{2+} level (Fig. 2e; Movie S4).

Interconnection of guard cells in stomata of ferns

In contrast to our experience with the stomata of seed plants *V. faba* and tobacco (Levchenko *et al.*, 2005; Marten *et al.*, 2007b; Voss *et al.*, 2016), we noticed that the calcium reporter dyes moved from the impaled guard cell into the adjacent cell in stomata of *A. scolopendrium* (Fig. 2e). The movement of fluorescent dyes from one to the other guard cell in a stomatal complex was also observed for the model fern species *C. richardii*, as well as the lycophyte *Selaginella unicinata* (Fig. S2). Stomata of ferns thus differ from those of dicotyledonous plants, as the cytosol of both guard cells in the complex is interconnected.

The nature of the cytosolic connections between guard cells in *P. vulgare* stomata was tested by current injection of Lucifer Yellow. This bright fluorescent Ca^{2+}-insensitive dye first appeared in the impaled guard cell (Fig. 3a; Movie S5), but, during the injection period of 20 min, also moved into the adjacent guard cell (Fig. 3b). The maximum intensity reached in the second cell was, on average, 0.6 times lower than the intensity observed in the current-injected guard cell. Similar results were obtained with *P. glycyrrhiza* (Fig. 3; Movie S6), which is one of the parental lines of the allotetraploid species *P. vulgare* (Haufler *et al.*, 1995). The slow movement of fluorescent dyes between the two guard cells is reminiscent of diffusion through plasmodesmata (Terry & Robards, 1987), which suggests that these cell wall-spanning pores connect guard cells in fern stomata.

In search for junctions between adjacent guard cells, electron microscopy images were obtained from the stomata of *P. glycyrrhiza*. These images showed that the nucleus in fern guard cells is localized at a central position of the guard cell (Fig. 4a), numerous chloroplasts surround the nucleus and vesicles are visible along the guard cell walls, which probably represent lipid droplets (Chapman *et al.*, 2012). A close examination of the cell wall between both guard cells showed that, indeed, a few long and narrow plasmodesmata are present, which interconnect the cytosol of these cells (Fig. 4b,c).

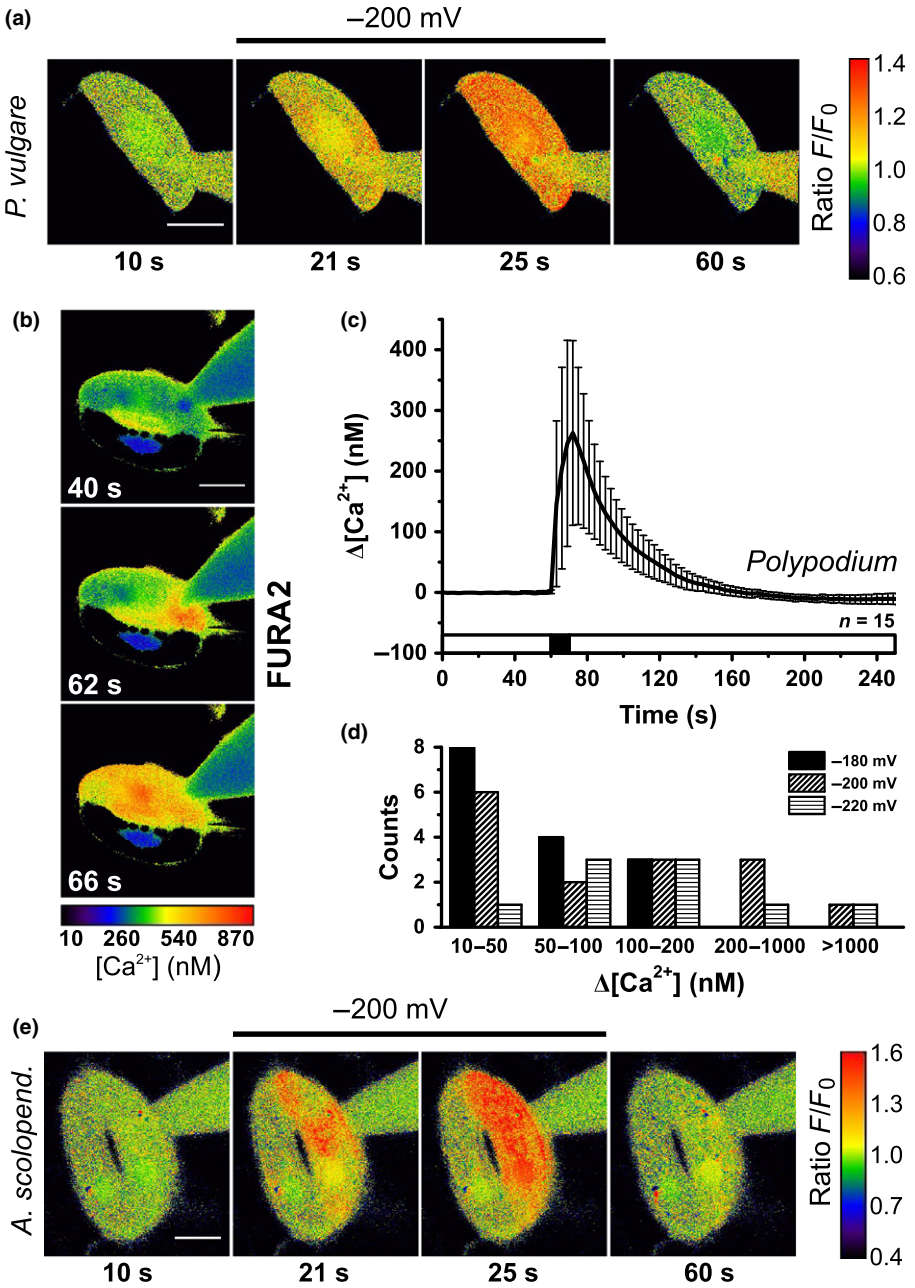

Fig. 2 Hyperpolarization-induced elevation of the cytosolic free Ca^{2+} concentration in fern guard cells. (a, e) Color-coded images of *Polypodium vulgare* (a) and *Asplenium scolopendrium* (e) guard cells showing changes in Oregon Green-BAPTA (OG-BAPTA) fluorescence intensity relative to the value measured at the start of the experiment. Images were obtained before (right panel), during (middle panels) and after clamping the membrane potential from −100 to −200 mV. The time from the start of the experiment is shown below each panel; bars, 20 μm. (b) Color-coded images of the cytosolic free Ca^{2+} concentration (based on FURA2 signals) in a *P. vulgare* guard cell, before (upper panel), during (middle panel) and after (lower panel) stimulation of the cell with a −200-mV voltage pulse. The color code is linked to cytosolic Ca^{2+} concentrations in the calibration bar below the panels and the time from the start of the experiment is indicated at the left bottom of each panel; bar, 20 μm. (c) Time-dependent changes in the cytosolic free Ca^{2+} concentration induced by a voltage pulse to −200 mV (indicated by the black area in the bar below the graph). Average data are shown for 15 *P. vulgare* guard cells; error bars, ± SE. (d) Frequency distribution of the magnitude of the rise in the cytosolic free Ca^{2+} concentration induced by voltage pulses to −180 (filled bars), −200 (diagonally striped bars) or −220 mV (horizontal striped bars). Data were obtained with FURA2-loaded *P. vulgare* guard cells as in (b) and (c).

Fern guard cells regulate their cytosolic Ca^{2+} level autonomously

The plasmodesmata between fern guard cells not only facilitate the exchange of fluorescent dyes, but may also provide a pathway for the exchange of ions, such as Ca^{2+}. We therefore tested whether Ca^{2+} signals triggered in one guard cell propagate into the neighboring cell. Stimulation of *P. vulgare* guard cells loaded with FURA2, with 10-s voltage pulses to −200 mV, evoked a strong increase in the cytosolic Ca^{2+} concentration in the impaled

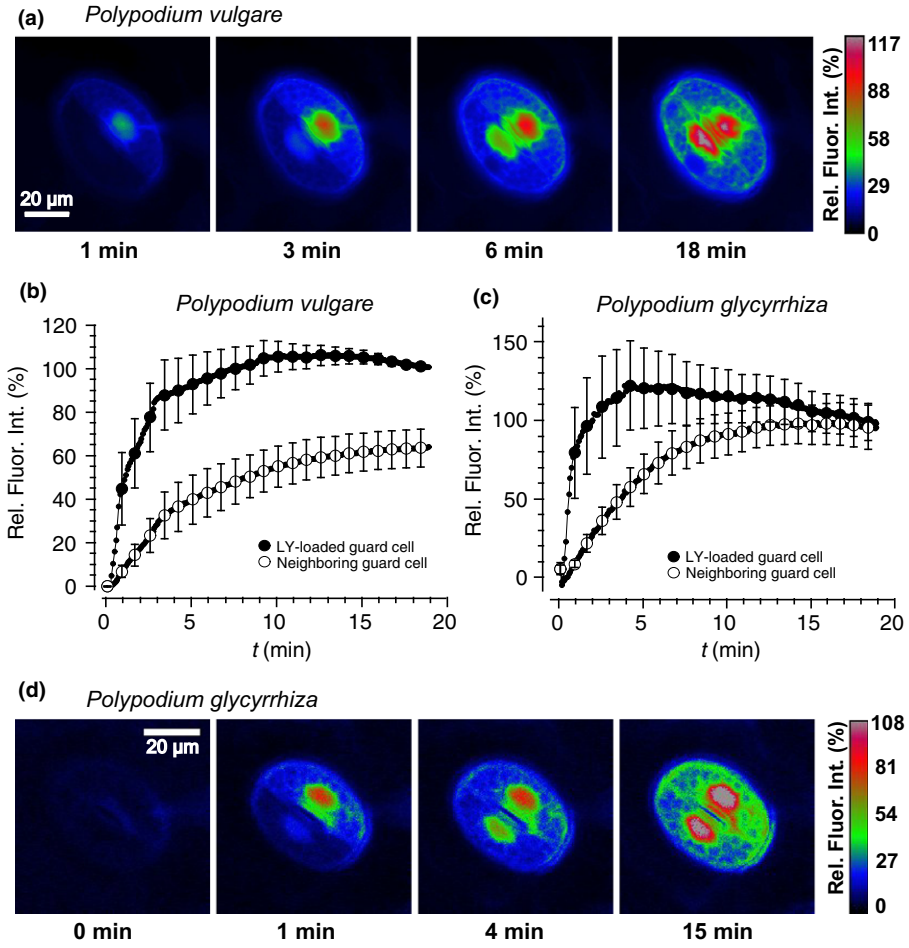

Fig. 3 Cytosolic connections between guard cells in fern stomata. (a, d) Color-coded images of *Polypodium vulgare* (a) and *Polypodium glycyrrhiza* (d) stomata for which the upper guard cell was current injected with Lucifer Yellow (LY). Note that, in time, the fluorescent dye moved into the lower (non-impaled) guard cell. The calibration bars on the right link the color code to the relative fluorescence intensity, which was set to 100% at the region of interest at $t = 20$ min. The time from the start of the experiments is shown below each panel. Bars, 20 µm. (b, c) Time-dependent increase in fluorescence intensity of LY current injected into a single guard cell (closed symbols) of fern stomata and slowly appearing in the neighboring guard cell (open symbols). Data are the average of 15 experiments with *P. vulgare* (b) and eight experiments with *P. glycyrrhiza* (c); error bars, ± SE.

guard cell (Fig. 5a; Movie S7), but caused only a minor Ca^{2+} elevation in the connected guard cell (Fig. 5b). On average, the change in the FURA2 ratio was 13 times higher in the voltage-stimulated cell relative to the neighboring guard cell (Fig. 5c). The strong differences in cytosolic Ca^{2+} signals between both guard cells lead to the following conclusions: (1) voltage pulses applied to one guard cell provoke membrane potential changes of a reduced magnitude in the neighboring cell; (2) the rate of Ca^{2+} diffusion between guard cells is low, despite the presence of plasmodesmata.

Although we observed only small spontaneous changes in the cytosolic Ca^{2+} concentration in *P. vulgare*, guard cells of *A. scolopendrium* displayed large repetitive Ca^{2+} transients (Fig. 6; Movie S8). These temporal modifications of the FURA2 ratio occurred in the non-impaled guard cells, and the period between the spikes ranged from 180 to 400 s. By contrast, only minor changes were found for the cytosolic free Ca^{2+} concentration of guard cells impaled with the microelectrode (Fig. 6).

Discussion

Guard cells of ferns are very similar to their relatives in seed plants with respect to the properties of voltage-dependent ion channels in the plasma membrane. The time-dependent activation of ion currents at membrane potentials positive and negative of −100 mV (Fig. 1) suggests that ferns have K^+-selective channels homologous to GORK and KAT1/2 of *Arabidopsis*. Within the framework of the 1000 Plants project (Matasci *et al.*, 2014), transcriptome data of various fern species have become available and can serve as an excellent starting point to explore the genes encoding shaker-type K^+ channels (Very & Sentenac, 2002; Hedrich, 2012). These studies will clarify whether voltage-dependent K^+ channels in guard cells are indeed evolutionarily conserved, as suggested by our measurements with microelectrodes.

Evolution of guard cell interconnections

Plasmodesmata between guard cells seem to have an early evolutionary origin, as they are found in stomata of the lycophyte *S. unicinata*, the aquatic fern *C. richardii* and the *Polypodiopsida*. These interconnections are likely to facilitate the diffusion of small osmotically active solutes, such as K^+, Cl^- and organic anions (Terry & Robards, 1987; Roberts & Oparka, 2003). Because of this ability, it is likely that plasmodesmata equilibrate the osmotic potential of guard cells in a stomatal complex and thus prevent imbalances in turgor.

The question arises as to why the symplastic connections between guard cells were lost during the evolution of seed plants

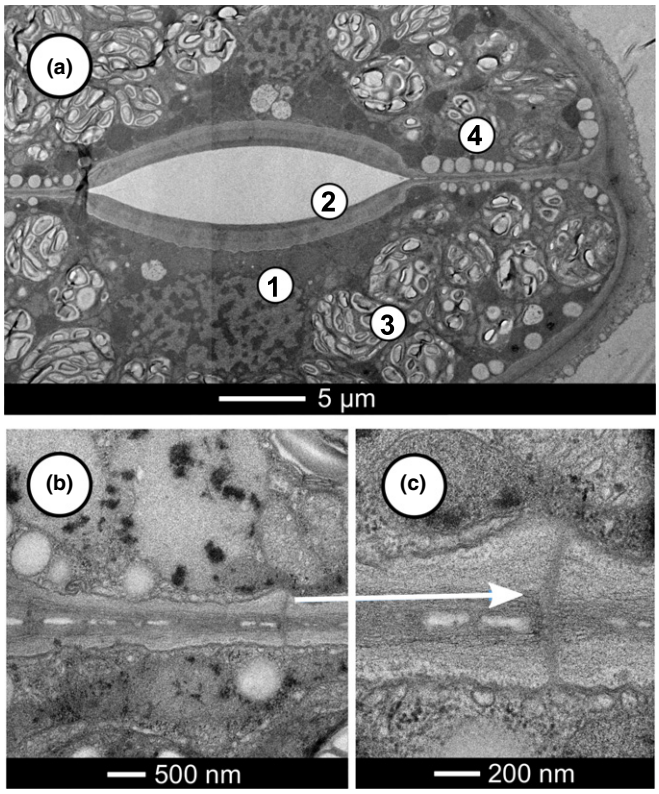

Fig. 4 Electron microscopy images of a *Polypodium glycyrrhiza* stoma. (a) Transverse section through a *P. glycyrrhiza* stoma; note that the nucleus (1) is located in the periphery of the guard cell, close to the stomatal split (2) and surrounded by multiple chloroplasts (3). Lipid droplets (4) are lined up in close proximity to the guard cell wall. (b, c) Close up of the cell wall interconnecting both guard cells; note the plasmodesma spanning the cell wall between the guard cells.

(Wille & Lucas, 1984; Palevitz & Hepler, 1985). Possibly, the presence of plasmodesmata that interconnect guard cells is linked to the mechanism by which these cells force stomatal opening. Whereas the stomata of ferns and mosses open through changes in the shape of the guard cell cross-section, guard cells in seed plants force stomatal opening by bending (Ziegler, 1987). It is conceivable that the larger degree of guard cell deformation in seed plants required higher turgor pressures and the equilibration of osmolarity between the guard cells was no longer required, which led to a loss of plasmodesmata during the evolution of seed plants.

Guard cells in a stomatal complex can also be interconnected through gaps in the cell walls, which are formed during the symmetrical division of the guard mother cell. An extreme case of such gaps is found for the moss *Funaria hygrometrica*, as the cell wall between guard cells is completely absent in this species (Sack & Paolillo, 1983, 1985). Gaps are also common in horsetails and grass species, which suggests that they have evolved independently in several plant clades (Brown & Johnson, 1962; Palevitz *et al.*, 1981; Sack, 1987). As the stomata of grasses open through relatively small changes in volume of the dumbbell-shaped guard cells, gaps in the cell wall may serve to prevent imbalances in turgor pressure and thereby to optimize stomatal movements (Franks & Farquhar, 2007; Mumm *et al.*, 2011; Chen *et al.*, 2017).

Does cytosolic coupling of guard cells affect Ca^{2+} signaling?

Despite the presence of plasmodesmata, the application of hyperpolarizing pulses to fern guard cells did not provoke cytosolic Ca^{2+} signals in the neighboring guard cell (Fig. 5). Apparently, the electrical conductance of the plasmodesmata is not high enough to provoke membrane potential changes in the non-impaled guard cell, which are sufficiently large to activate Ca^{2+}-permeable channels. Future studies with microelectrodes in both guard cells of a fern stomatal complex may reveal the electrical conductance of plasmodesmata and show whether these pores are regulated by physiological signals, such as changes in the cytosolic Ca^{2+} concentration.

In addition to the limited electrical conductance, the plasmodesmata between fern guard cells are also unlikely to facilitate rapid diffusion of Ca^{2+}, which would equilibrate the free cytosolic Ca^{2+} concentration of both cells. This is evident from the measurements with *A. scolopendrium* stomata, in which the Ca^{2+} level of one guard cell remains relatively stable, whereas the other shows trains of Ca^{2+} transients (Fig. 6). Apparently, individual guard cells in fern stomatal complexes are able to control their cytosolic Ca^{2+} signals autonomously. Unlike ferns, the guard cells of grasses are connected by gaps in the cell wall (Palevitz *et al.*, 1981), which enable a rapid exchange of fluorescent dyes (Mumm *et al.*, 2011). It is therefore likely that guard cells of grasses have a uniform membrane potential and that Ca^{2+} signals can propagate from one cell to the other.

Outlook

Whereas the properties of voltage-dependent K^+ channels are likely to have been conserved during evolution, Ca^{2+}-dependent responses may vary. In guard cells of *A. scolopendrium*, we measured repetitive transient elevations of cytosolic Ca^{2+}, which resemble those reported previously for guard cells of *Commelina communis* and *Arabidopsis* (McAinsh *et al.*, 1995; Allen *et al.*, 2001; Hetherington & Brownlee, 2004). These oscillations were not observed in the cells loaded with FURA2, which may be a result of the higher concentration of the Ca^{2+} buffer FURA2, or the constant membrane potential of −100 mV, to which these cells were clamped. No trains of Ca^{2+} signals were observed in the guard cells of *P. vulgare* (Fig. 5b), even though this species belongs to the same order of Polypodiales as *A. scolopendrium*. These differences in Ca^{2+} homeostasis between related species suggests that the mechanisms involved in Ca^{2+} signaling can rapidly change during evolution, which may be linked to the large numbers of gene families that are involved in these signal transduction pathways (Wheeler & Brownlee, 2008; Dodd *et al.*, 2010; Edel *et al.*, 2017). An in-depth comparison of related and more distant plant species may therefore shed light into the evolution of genes that are involved in the generation and encoding of signals provided by this universal second messenger.

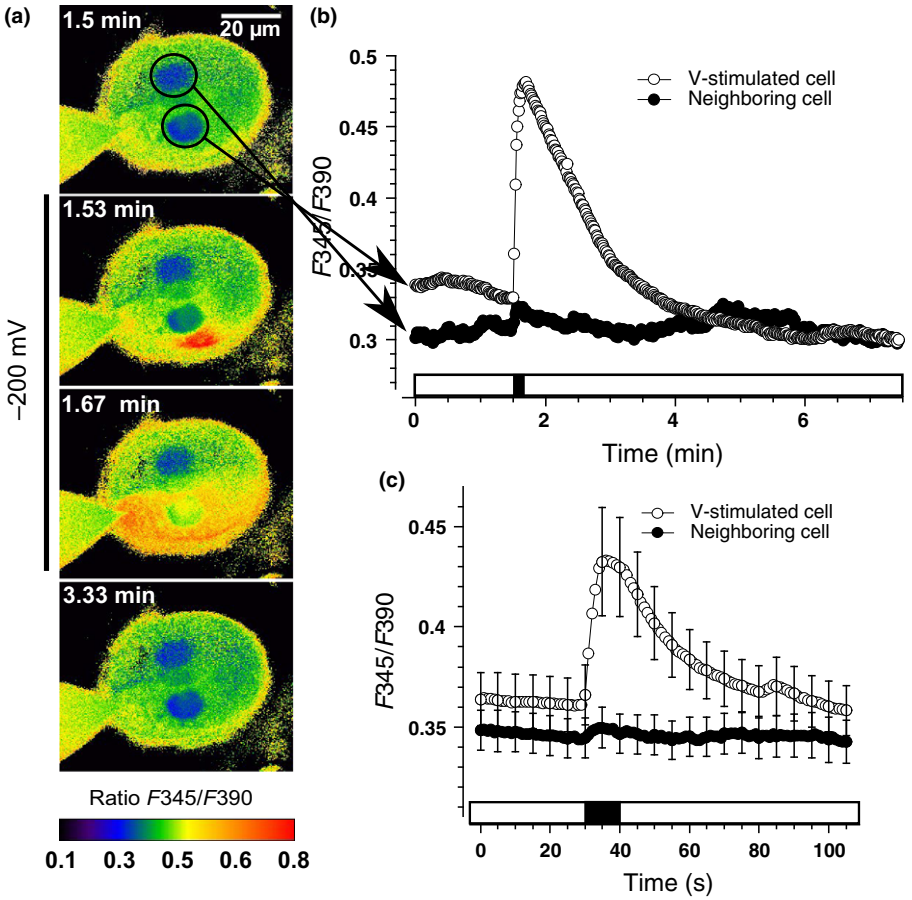

Fig. 5 Voltage-induced Ca^{2+} signals are not transmitted between guard cells in fern stomata. (a) Color-coded images representing the FURA2 ratio signal in a *Polypodium vulgare* stoma, in which the lower guard cell was stimulated with a −200-mV voltage pulse. The images were obtained before (upper panel), during (middle panels) and after (lower panel) the −200-mV voltage pulse. The time after the start of the experiment is shown in the upper left corner of each image. The calibration bar below the images links the color code to the FURA2 *F*345/*F*390 ratio. Black circles in (a) indicate the regions of interest (ROIs) that were used to determine time-dependent changes in the FURA2 ratio signal, as shown in (b). (b) Arrows link the ROIs in (a) to the traces of the guard cell stimulated with the voltage pulse (open symbols) and in the neighboring guard cell (closed symbols). The dark area of the bar below the graph shows the period at which the −200-mV pulse was applied. (c) Time-dependent changes in the FURA2 ratio signal induced by −200-mV voltage pulses, as in (b), but averaged for 22 *P. vulgare* stomata. Error bars, ± SE.

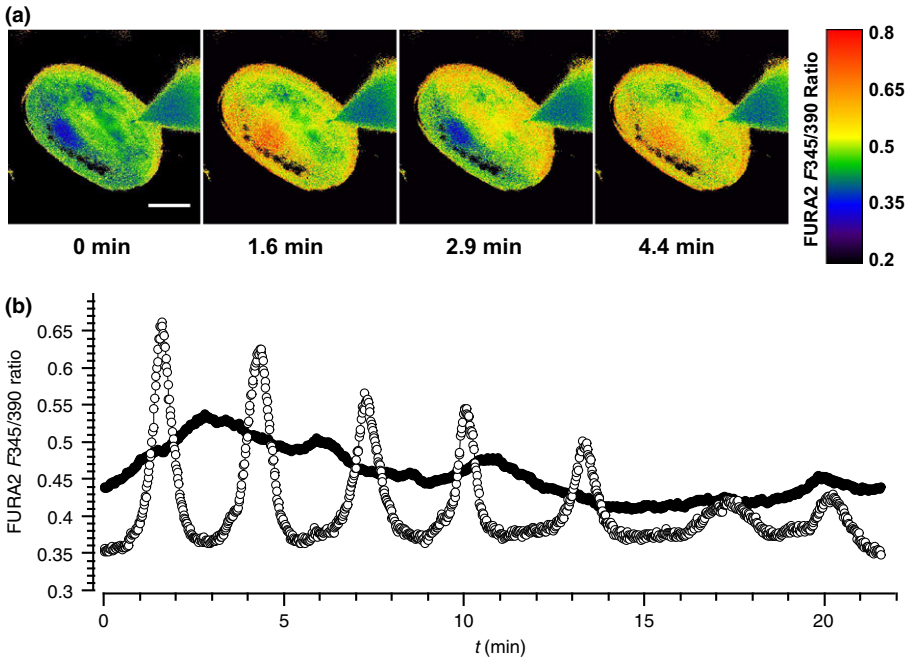

Fig. 6 Repetitive rises in the cytosolic free Ca^{2+} concentration of *Asplenium scolopendrium* guard cells. (a) Color-coded images representing the FURA2 *F*345/*F*390 ratio signal of an *A. scolopendrium* stoma for which the upper guard cell was current injected with FURA2, which moved into the lower guard cell. The images were obtained at the time points indicated below the panels. The color code is linked to the FURA2 ratio in the calibration bar on the right. Note that the cytosolic free Ca^{2+} concentration of the lower cell changes repetitively, whereas that of the upper cell remains virtually stable. (b) Time-dependent changes of the FURA2 ratio signal shown for the same stoma as in (a). Data were obtained for a region of interest at the periphery of the upper (closed symbols) and lower (open symbols) guard cells. Scale bar, 20 µm.

Acknowledgements

We thank Erin Sigel, University of Louisiana, for information concerning the phylogenetic relations of ferns, and Alistair Hetherington, University of Bristol, for providing *Selaginella unicinata* plants. This work was supported by grants from the German Research Foundation (DFG) in the project 'Evolution of molecular mechanisms that control stomatal closure'

(RO2381/8-1 and HE1640/40-1), awarded to R.H. and M.R.G.R., and Australian Research Council grants DE140 100946 to S.A.M.M. and DP140100666 to T.B. We thank the Franceschi Microscopy and Imaging Center at Washington State University for technical support.

Author contributions

L.J.V., S.A.M.M., T.B., R.H. and M.R.G.R. planned and designed the research; L.J.V., S.A.M.M., M.K., J.M.R. and M.R.G.R. performed the experiments; L.J.V., M.K., J.M.R. and M.R.G.R. conducted the data analysis; S.A.M.M., T.B., R.H. and M.R.G.R. wrote the manuscript.

References

Ache P, Becker D, Ivashikina N, Dietrich P, Roelfsema MRG, Hedrich R. 2000. GORK, a delayed outward rectifier expressed in guard cells of *Arabidopsis thaliana*, is a K^+-selective, K^+-sensing ion channel. *FEBS Letters* **486**: 93–98.

Allen GJ, Chu SP, Harrington CL, Schumacher K, Hoffman T, Tang YY, Grill E, Schroeder JI. 2001. A defined range of guard cell calcium oscillation parameters encodes stomatal movements. *Nature* **411**: 1053–1057.

Bauer H, Ache P, Lautner S, Fromm J, Hartung W, Al-Rasheid KAS, Sonnewald S, Sonnewald U, Kneitz S, Lachmann N *et al.* 2013. The stomatal response to reduced relative humidity requires guard cell-autonomous ABA synthesis. *Current Biology* **23**: 53–57.

Berry JA, Beerling DJ, Franks PJ. 2010. Stomata: key players in the earth system, past and present. *Current Opinion in Plant Biology* **13**: 232–239.

Brodribb TJ, McAdam SAM. 2011. Passive origins of stomatal control in vascular plants. *Science* **331**: 582–585.

Brodribb TJ, McAdam SAM. 2017. Evolution of the stomatal regulation of plant water content. *Plant Physiology* **174**: 639–649.

Brodribb TJ, McAdam SAM, Jordan GJ, Feild TS. 2009. Evolution of stomatal responsiveness to CO_2 and optimization of water-use efficiency among land plants. *New Phytologist* **183**: 839–847.

Brown WV, Johnson SC. 1962. The fine structure of grass guard cell. *American Journal of Botany* **49**: 110–115.

Cai SG, Chen G, Wang YY, Huang YQ, Marchant DB, Wang YZ, Yang Q, Dai F, Hills A, Franks PJ *et al.* 2017. Evolutionary conservation of ABA signaling for stomatal closure. *Plant Physiology* **174**: 732–747.

Chapman KD, Dyer JM, Mullen RT. 2012. Biogenesis and functions of lipid droplets in plants. *Journal of Lipid Research* **53**: 215–226.

Chater C, Caine RS, Tomek M, Wallace S, Kamisugi Y, Cuming AC, Lang D, MacAlister CA, Casson S, Bergmann DC *et al.* 2016. Origin and function of stomata in the moss *Physcomitrella patens*. *Nature Plants* **2**: 16179.

Chater C, Kamisugi Y, Movahedi M, Fleming A, Cuming AC, Gray JE, Beerling DJ. 2011. Regulatory mechanism controlling stomatal behavior conserved across 400 million years of land plant evolution. *Current Biology* **21**: 1025–1029.

Chen ZH, Chen G, Dai F, Wang YZ, Hills A, Ruan YL, Zhang GP, Franks PJ, Nevo E, Blatt MR. 2017. Molecular evolution of grass stomata. *Trends in Plant Science* **22**: 124–139.

Dodd AN, Kudla J, Sanders D. 2010. The language of calcium signaling. *Annual Review of Plant Biology* **61**: 593–620.

Doi M, Kitagawa Y, Shimazaki K. 2015. Stomatal blue light response is present in early vascular plants. *Plant Physiology* **169**: 1205–1213.

Doi M, Shimazaki KI. 2008. The stomata of the fern *Adiantum capillus-veneris* do not respond to CO_2 in the dark and open by photosynthesis in guard cells. *Plant Physiology* **147**: 922–930.

Duckett JG, Pressel S. 2018. The evolution of the stomatal apparatus: intercellular spaces and sporophyte water relations in bryophytes—two ignored dimensions. *Philosophical Transactions of the Royal Society B: Biological Sciences* **373**: 20.

Edel KH, Marchadier E, Brownlee C, Kudla J, Hetherington AM. 2017. The evolution of calcium-based signalling in plants. *Current Biology* **27**: R667–R679.

Franks PJ, Britton-Harper ZJ. 2016. No evidence of general CO_2 insensitivity in ferns: one stomatal control mechanism for all land plants? *New Phytologist* **211**: 819–827.

Franks PJ, Farquhar GD. 2007. The mechanical diversity of stomata and its significance in gas-exchange control. *Plant Physiology* **143**: 78–87.

Grabov A, Blatt MR. 1998. Membrane voltage initiates Ca^{2+} waves and potentiates Ca^{2+} increases with abscisic acid in stomatal guard cells. *Proceedings of the National Academy of Sciences, USA* **95**: 4778–4783.

Grynkiewicz G, Poenie M, Tsien RY. 1985. A new generation of Ca^{2+} indicators with greatly improved fluorescence properties. *Journal of Biological Chemistry* **260**: 3440–3450.

Hamilton DWA, Hills A, Kohler B, Blatt MR. 2000. Ca^{2+} channels at the plasma membrane of stomatal guard cells are activated by hyperpolarization and abscisic acid. *Proceedings of the National Academy of Sciences, USA* **97**: 4967–4972.

Haufler CH, Windham MD, Rabe EW. 1995. Reticulate evolution in the *Polypodium vulgare* complex. *Systematic Botany* **20**: 89–109.

Hedrich R. 2012. Ion channels in plants. *Physiological Reviews* **92**: 1777–1811.

Hetherington AM, Brownlee C. 2004. The generation of Ca^{2+} signals in plants. *Annual Review of Plant Biology* **55**: 401–427.

Hetherington AM, Woodward FI. 2003. The role of stomata in sensing and driving environmental change. *Nature* **424**: 901–908.

Hiyama A, Takemiya A, Munemasa S, Okuma E, Sugiyama N, Tada Y, Murata Y, Shimazaki K. 2017. Blue light and CO_2 signals converge to regulate light-induced stomatal opening. *Nature Communications* **8**: 13.

Horak H, Kollist H, Merilo E. 2017. Fern stomatal responses to ABA and CO_2 depend on species and growth conditions. *Plant Physiology* **174**: 672–679.

Kim TH, Bohmer M, Hu HH, Nishimura N, Schroeder JI. 2010. Guard cell signal transduction network: advances in understanding abscisic acid, CO_2, and Ca^{2+} signaling. *Annual Review of Plant Biology* **61**: 561–591.

Kollist H, Nuhkat M, Roelfsema MRG. 2014. Closing gaps: linking elements that control stomatal movement. *New Phytologist* **203**: 44–62.

Kudla J, Batistic O, Hashimoto K. 2010. Calcium signals: the lead currency of plant information processing. *Plant Cell* **22**: 541–563.

Levchenko V, Guinot DR, Klein M, Roelfsema MRG, Hedrich R, Dietrich P. 2008. Stringent control of cytoplasmic Ca^{2+} in guard cells of intact plants compared to their counterparts in epidermal strips or guard cell protoplasts. *Protoplasma* **233**: 61–72.

Levchenko V, Konrad KR, Dietrich P, Roelfsema MRG, Hedrich R. 2005. Cytosolic abscisic acid activates guard cell anion channels without preceding Ca^{2+} signals. *Proceedings of the National Academy of Sciences, USA* **102**: 4203–4208.

Lösch R, Bressel C. 1979. Guard cell potassium relations in Leptosporangiate ferns showing diverse types of stomata. *Flora* **168**: 109–120.

Marten H, Hedrich R, Roelfsema MRG. 2007a. Blue light inhibits guard cell plasma membrane anion channels in a phototropin-dependent manner. *Plant Journal* **50**: 29–39.

Marten H, Konrad KR, Dietrich P, Roelfsema MRG, Hedrich R. 2007b. Ca^{2+}-dependent and -independent abscisic acid activation of plasma membrane anion channels in guard cells of *Nicotiana tabacum*. *Plant Physiology* **143**: 28–37.

Matasci N, Hung L-H, Yan Z, Carpenter EJ, Warnow T, Ayyampalayam S, Barker M, Burleigh JG, Gitzendanner MA, Wafula E *et al.* 2014. Data access for the 1,000 Plants (1KP) project. *GigaScience* **3**: 1–10.

McAdam SAM, Brodribb TJ. 2012. Fern and lycophyte guard cells do not respond to endogenous abscisic acid. *Plant Cell* **24**: 1510–1521.

McAinsh MR, Webb AAR, Taylor JE, Hetherington AM. 1995. Stimulus-induced oscillations in guard-cell cytosolic-free calcium. *Plant Cell* **7**: 1207–1219.

Mumm P, Wolf T, Fromm J, Roelfsema MRG, Marten I. 2011. Cell type-specific regulation of ion channels within the maize stomatal complex. *Plant and Cell Physiology* **52**: 1365–1375.

Palevitz BA, Hepler PK. 1985. Changes in dye coupling of stomatal cells of *Allium* and *Commelina* demonstrated by microinjection of lucifer yellow. *Planta* **164**: 473–479.

Palevitz BA, Okane DJ, Kobres RE, Raikhel NV. 1981. The vacuole system in stomatal cells of *Allium* – vacuole movements and changes in morphology in differentiating cells as revealed by epifluorescence, video and electron-microscopy. *Protoplasma* **109**: 23–55.

Pei ZM, Murata Y, Benning G, Thomine S, Klusener B, Allen GJ, Grill E, Schroeder JI. 2000. Calcium channels activated by hydrogen peroxide mediate abscisic acid signalling in guard cells. *Nature* **406**: 731–734.

Raven JA, Edwards D. 2014. Photosynthesis in early land plants: adapting to the terrestrial environment. In: Hanson DT, Rice SK, eds. *Photosynthesis in bryophytes and early land plants*. Dordrecht, Netherlands: Springer, 29–58.

Roberts AG, Oparka KJ. 2003. Plasmodesmata and the control of symplastic transport. *Plant, Cell & Environment* **26**: 103–124.

Roelfsema MRG, Hanstein S, Felle HH, Hedrich R. 2002. CO_2 provides an intermediate link in the red light response of guard cells. *Plant Journal* **32**: 65–75.

Roelfsema MRG, Hedrich R. 2005. In the light of stomatal opening: new insights into 'the Watergate'. *New Phytologist* **167**: 665–691.

Roelfsema MRG, Hedrich R. 2010. Making sense out of Ca^{2+} signals: their role in regulating stomatal movements. *Plant, Cell & Environment* **33**: 305–321.

Roelfsema MRG, Hedrich R. 2016. Do stomata of evolutionary distant species differ in sensitivity to environmental signals? *New Phytologist* **211**: 767–770.

Roelfsema MRG, Konrad KR, Marten H, Psaras GK, Hartung W, Hedrich R. 2006. Guard cells in albino leaf patches do not respond to photosynthetically active radiation, but are sensitive to blue light, CO_2 and abscisic acid. *Plant, Cell & Environment* **29**: 1595–1605.

Ruszala EM, Beerling DJ, Franks PJ, Chater C, Casson SA, Gray JE, Hetherington AM. 2011. Land plants acquired active stomatal control early in their evolutionary history. *Current Biology* **21**: 1030–1035.

Sack FD. 1987. The development and structure of stomata. In: Zeiger E, Farquhar GD, Cowan IR, eds. *Stomatal function*. Stanford, CA, USA: Stanford University Press, 59–90.

Sack F, Paolillo DJ. 1983. Structure and development of walls in *Funaria* stomata. *American Journal of Botany* **70**: 1019–1030.

Sack FD, Paolillo DJ. 1985. Incomplete cytokinesis in *Funaria* stomata. *American Journal of Botany* **72**: 1325–1333.

Shimazaki KI, Doi M, Assmann SM, Kinoshita T. 2007. Light regulation of stomatal movement. *Annual Review of Plant Biology* **58**: 219–247.

Stange A, Hedrich R, Roelfsema MRG. 2010. Ca^{2+}-dependent activation of guard cell anion channels, triggered by hyperpolarization, is promoted by prolonged depolarization. *Plant Journal* **62**: 265–276.

Stevens RA, Martin ES. 1977. New structure associated with stomatal complex of fern *Polypodium vulgare*. *Nature* **265**: 331–334.

Szyroki A, Ivashikina N, Dietrich P, Roelfsema MRG, Ache P, Reintanz B, Deeken R, Godde M, Felle H, Steinmeyer R *et al.* 2001. KAT1 is not essential for stomatal opening. *Proceedings of the National Academy of Sciences, USA* **98**: 2917–2921.

Terry BR, Robards AW. 1987. Hydrodynamic radius alone governs the mobility of molecules through plasmodesmata. *Planta* **171**: 145–157.

Very AA, Sentenac H. 2002. Cation channels in the Arabidopsis plasma membrane. *Trends in Plant Science* **7**: 168–175.

Voss LJ, Hedrich R, Roelfsema MRG. 2016. Current injection provokes rapid expansion of the guard cell cytosolic volume and triggers Ca^{2+} signals. *Molecular Plant* **9**: 471–480.

Wheeler GL, Brownlee C. 2008. Ca^{2+} signalling in plants and green algae – changing channels. *Trends in Plant Science* **13**: 506–514.

Wille AC, Lucas WJ. 1984. Ultrastructural and histochemical-studies on guard cells. *Planta* **160**: 129–142.

Ziegler H. 1987. The evolution of stomata. In: Zeiger E, Farquhar GD, Cowan IR, eds. *Stomatal function*. Stanford, CA, USA: Stanford University Press, 29–58.

Supporting Information

Additional Supporting Information may be found online in the Supporting Information tab for this article:

Fig. S1 Hyperpolarization-induced elevation of the cytosolic free Ca^{2+} concentration in a *Polypodium vulgare* guard cell and bright field images of *P. vulgare* and *Asplenium scolopendrium* stomata.

Fig. S2 False colored images of stomata of *Ceratopteris richardii* and *Selaginella uncinata* loaded with FURA2 via the guard cells on the right.

Movie S1 Changes in the Oregon Green-BAPTA fluorescence intensity in a *Polypodium vulgare* guard cell stimulated with a 10-s voltage pulse from −100 to −200 mV.

Movie S2 Changes in the cytosolic free Ca^{2+} concentration, which start close to the site of impalement, in a *Polypodium vulgare* guard cell stimulated with a 10-s voltage pulse from −100 to −200 mV.

Movie S3 Changes in the cytosolic free Ca^{2+} concentration, which start away from the site of impalement, in a *Polypodium vulgare* guard cell stimulated with a 10-s voltage pulse from −100 to −200 mV.

Movie S4 Changes in the Oregon Green-BAPTA fluorescence intensity in an *Asplenium scolopendrium* guard cell stimulated with a 10-s voltage pulse from −100 to −200 mV.

Movie S5 Color-coded movie of a *Polypodium vulgare* stoma for which the upper guard cell was current injected with Lucifer Yellow.

Movie S6 Color-coded movie of a *Polypodium glycyrrhiza* stoma for which the upper guard cell was current injected with Lucifer Yellow.

Movie S7 *Polypodium vulgare* stoma for which the upper guard cell was stimulated with a 10-s voltage pulse to −200 mV, which evoked a transient rise in the FURA2 *F*345/*F*390 ratio of the stimulated cell, whereas that of the neighboring guard cell remained stable.

Movie S8 Spontaneous changes in the cytosolic free Ca^{2+} concentration in an *Asplenium scolopendrium* guard cell.

Please note: Wiley Blackwell are not responsible for the content or functionality of any Supporting Information supplied by the authors. Any queries (other than missing material) should be directed to the *New Phytologist* Central Office.